

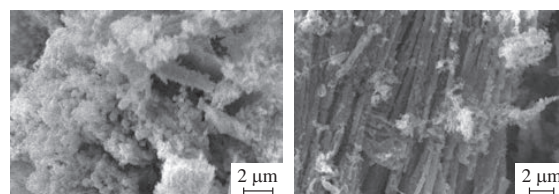
## Synthesis, structure, optical and photocatalytic properties of copper-activated ZnO

Olga I. Gyrdasova,\* Marina A. Melkozerova, Inna V. Baklanova, Larisa Yu. Buldakova, Natalya S. Sycheva, Vladimir N. Krasil'nikov and Mikhail Yu. Yanchenko

*Institute of Solid State Chemistry, Ural Branch of the Russian Academy of Sciences, 620990 Ekaterinburg, Russian Federation. Fax: +7 343 374 4495; e-mail: Gyrdasova@ihim.uran.ru*

DOI: 10.1016/j.mencom.2017.07.032

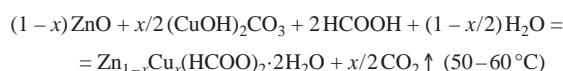
**The  $Zn_{1-x}Cu_xO$  ( $0 < x \leq 0.1$ ) solid solutions and  $Zn_{1-x}Cu_xO:CuO$  composite materials have been synthesized by a precursor technology using  $Zn_{1-x}Cu_x(HCOO)_2 \cdot 2H_2O$  ( $0 < x \leq 0.2$ ) mixed formates as precursors, and their structural, optical and photocatalytic characteristics have been ascertained.**



Nanodispersed zinc oxide (ZnO) has been extensively studied in connection with its practical applications in solar cells, photo-detectors, field emission cathodes, ferromagnetic materials and photocatalysts for the deep oxidation of toxic organic substances.<sup>1–4</sup> However, a considerable rate of electron-hole recombination and photoactivity predominantly in the ultraviolet range with a low quantum yield substantially constrain the application of ZnO as a photocatalyst. The photoactivity of such materials can be increased and displaced into the visible spectrum region by doping, changing the accessible surface size and morphology of aggregates and enhancing the degree of intrinsic defectiveness.<sup>4,5</sup> In our opinion, a precursor technology based on the thermolysis of zinc complexes with organic ligands is the most promising method for the synthesis of this material, which makes it possible to control both the microstructural characteristics of ZnO and the degree of its intrinsic defectiveness. The advantage of this method is that any compounds capable of transforming into oxides on heating can be used as precursors. Earlier, the solid solutions  $Zn_{1-x}Cu_xO$  with tubular particle morphology have been synthesized employing this technology from mixed formate glycolates of the general formula  $Zn_{1-x}Cu_x(HCOO)(OCH_2CH_2O)_{1/2}$ ; these solid solutions exhibited a high photocatalytic activity in the oxidation of hydroquinone in visible light.<sup>6,7</sup> Copper as an alloying addition is an effective acceptor impurity influencing the electronic band structure and intrinsic defectiveness of ZnO.<sup>8,9</sup> Since the catalytic activity of CuO in the oxidation of organic substances is well known,<sup>10</sup> it is interesting to obtain a catalyst based on the solid solution  $Zn_{1-x}Cu_xO$  with a copper oxide modified surface. The use of nanostructured hybrid shells in such photoelectrochemical systems provides additional possibility to affect the electron and hole dynamics and the bandgap width of a ZnO matrix.

In this work, in order to produce  $Zn_{1-x}Cu_xO$  solid solutions and nanodispersed  $Zn_{1-x}Cu_xO:CuO$  composite materials with an extended optical range of catalytic activity, we have developed a method in which the mixed formate  $Zn_{1-x}Cu_x(HCOO)_2 \cdot 2H_2O$  was used as a precursor. This compound is a product of isomorphous substitution of copper for a part of zinc in the structure of  $Zn(HCOO)_2 \cdot 2H_2O$ .

The formate  $Zn_{1-x}Cu_x(HCOO)_2 \cdot 2H_2O$  was produced under solvothermal conditions by the reaction



According to the XPS, IR spectroscopic and scanning electron microscopic data, the mixed formate  $Zn_{1-x}Cu_x(HCOO)_2 \cdot 2H_2O$  ( $0 < x \leq 0.2$ ) is an individual compound crystallizing as light blue scaly crystals with an average particle size of 50 nm in the region of existence of solid solutions between the  $Zn(HCOO)_2 \cdot 2H_2O$ – $Cu(HCOO)_2 \cdot 2H_2O$  system components. The X-ray phase analysis of the products of  $Zn_{1-x}Cu_x(HCOO)_2 \cdot 2H_2O$  thermolysis in air at 450 °C revealed that the monophasic solid solutions  $Zn_{1-x}Cu_xO$  with a wurtzite structure are formed at  $0 < x \leq 0.1$ . Along with the basic phase  $Zn_{1-x}Cu_xO$ , the samples with  $x > 0.1$  contain the diffraction lines of a CuO impurity phase.

In accordance with the scanning electron microscopy (SEM) data (JSM-6390 LA, JEOL), the  $Zn_{1-x}Cu_x(HCOO)_2 \cdot 2H_2O$  thermolysis products are quasi-one-dimensional polycrystals ready to longitudinal intergrowth (Figure 1). At high magnifications, it is seen that the surface of the aggregates has a hierarchical structure of smaller crystallites. The introduction of Cu into the zinc formate sample forwards a transition to linear structures. The initial zinc formate is an unstructured polycrystalline substance. We observed a tendency to elongate the fibers in aggregates as the concentration of copper in the samples increased. Reflected electron imaging (BSE mode) reveals a monochrome distribution of X-ray contrast, which is typical of the structure of composites

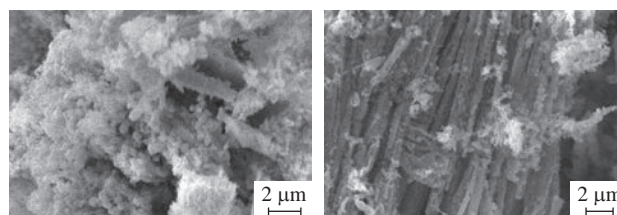


**Figure 1** The SEM image of the morphology of particles of  $Zn_{1-x}Cu_xO$ , where  $x$  is (a) 0.05 and (b) 0.2.

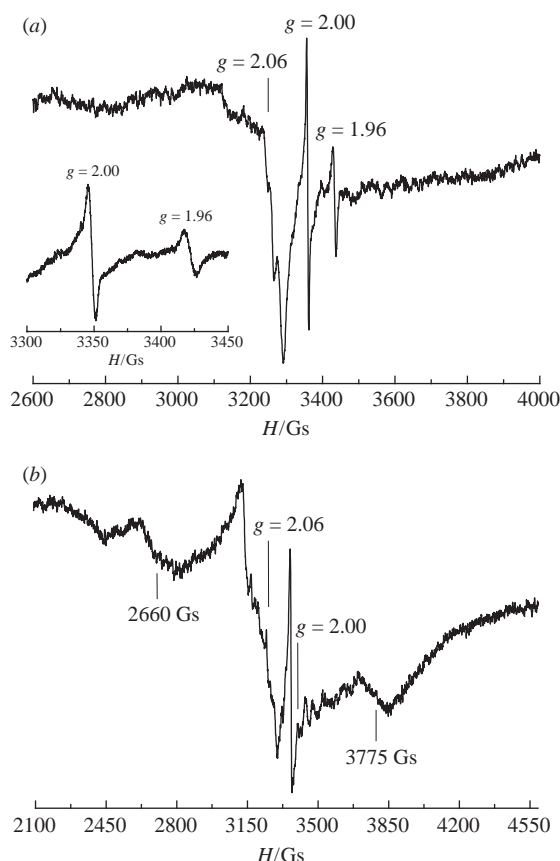


**Figure 2** EPR spectra of (a)  $\text{Zn}_{0.95}\text{Cu}_{0.05}\text{O}$  and (b)  $\text{Zn}_{0.8}\text{Cu}_{0.2}\text{O}$  samples.

in which CuO is distributed on the  $\text{Zn}_{1-x}\text{Cu}_x\text{O}$  nucleus as a uniform surface layer. The data of energy-dispersive X-ray (EDX) analysis, elemental analysis by atomic absorption spectrometry (Perkin-Elmer) in acetylene–air flame and inductively coupled plasma atomic emission spectrometry (JY-48) showed that the composition of the samples  $\text{Zn}_{0.8}\text{Cu}_{0.2}\text{O}$  corresponded to that conventionally ascribed to this compound.

The X-band EPR spectra (CMS-8400, ADANY) of the solid solutions  $\text{Zn}_{1-x}\text{Cu}_x\text{O}$  ( $x = 0.05, 0.1$ ), measured at room temperature, exhibit two narrow symmetrical lines with  $g$ -factors of 2.00 ( $\Delta H_{\text{pp}} = 5$  Gs) and 1.96 ( $\Delta H_{\text{pp}} = 8$  Gs) (Figure 2). According to the literature data, the line with the  $g$ -factor close to the spin value in wurtzite belongs to single-charged oxygen vacancies  $V_{\text{O}}^+$ .<sup>11,12</sup> The high-field signal with  $g = 1.96$  is attributed to electrons on shallow donor levels; as a rule, it is due to the presence of impurities such as iron in the structure.<sup>13</sup> The relative intensity of this signal decreased with the concentration of copper in the samples, probably, due to the reduction of the occupancy of impurity levels as a result of electron capture by  $\text{Cu}^{2+}$  ions and the transition of copper into a monovalent state. In addition to the above signals, the spectra of the samples also exhibited a broad asymmetrical signal ( $\Delta H_{\text{pp}} \approx 100$  Gs) with an absorption maximum corresponding to a  $g$ -factor of 2.06, which is ascribed to the  $\text{Cu}^{2+}$  ions (electron configuration  $d^9$ ) in the tetrahedral positions of wurtzite. The asymmetrical shape of the lines caused by the distribution of spectroscopic parameters is indicative of a disorder in the local environment of copper in the samples of  $\text{Zn}_{1-x}\text{Cu}_x\text{O}$  ( $x = 0.05, 0.1$ ).<sup>14</sup>

The spectrum of the  $\text{Zn}_{0.8}\text{Cu}_{0.2}\text{O}$  sample containing CuO is different from the spectra of the solid solutions. First, there is no line with  $g = 1.96$  in the spectrum of  $\text{Zn}_{0.8}\text{Cu}_{0.2}\text{O}$ . Second, along with the lines from oxygen vacancies  $V_{\text{O}}^+$  and  $\text{Cu}^{2+}$  ions, broad ( $\Delta H_{\text{pp}} \approx 150$  Gs) low-intensity lines at 2660 and 3775 Gs are observed in this spectrum. These signals are the fine structure

lines of  $\text{Fe}^{3+}$  ions (electron configuration  $d^5$ ) located in the diamagnetic matrix of ZnO.<sup>13</sup> In this case, the uncontrollable iron impurity was introduced into the sample during synthesis. Since all of the samples were produced under the same conditions, the signal with  $g = 1.96$  in the spectra of  $\text{Zn}_{1-x}\text{Cu}_x\text{O}$  ( $x = 0.05, 0.1$ ) is likely due to the presence of iron forming the impurity levels in the region of shallow donors. The absence of this signal, on the one hand, and the appearance of the  $\text{Fe}^{3+}$  fine structure lines in the spectrum of the  $\text{Zn}_{0.8}\text{Cu}_{0.2}\text{O}$  composite, on the other hand, are indicative of the effect of CuO on the electronic structure of wurtzite, and they suggest the occurrence of contact phenomena between the ZnO matrix and the copper oxide layer covering this matrix. This result shows that the sample of the general composition  $\text{Zn}_{0.8}\text{Cu}_{0.2}\text{O}$  is a nucleus-shell type composite material rather than a mechanical mixture of  $\text{Zn}_{1-x}\text{Cu}_x\text{O}$  and CuO phases.

To determine the effect of copper on the absorption of zinc oxide, we have examined the UV, visible and NIR absorption spectra of the samples, which were measured in a range of 220–1400 nm (UV-3600 spectrometer, Shimadzu,  $\lambda = 310$  nm) using  $\text{BaSO}_4$  as a reference. In the spectra of the solid solutions  $\text{Zn}_{1-x}\text{Cu}_x\text{O}$  ( $x = 0.05, 0.1$ ) and the  $\text{Zn}_{0.8}\text{Cu}_{0.2}\text{O}$  composite, the absorption band edge was not displaced into the long wavelength region relative to pure ZnO (Figure 3). The bandgap width of the solid solutions determined by the extrapolation of an absorption spectrum straight-line portion represented as  $(ah\nu)^2 = f(h\nu)$  until intersection with the abscissa axis is 3.15 eV. The bandgap of copper oxide obtained by the thermolysis of copper formate  $\text{Cu}(\text{HCOO})_2$  is 1.5 eV. The  $\text{Cu}^{2+}$  cations in CuO are characterized by a broad absorption band with a maximum at 600 nm, which is due to the  $d-d$  transition  ${}^2T_{2g} \rightarrow {}^2E_g$ . In the UV range, there is an absorption band at 270 nm corresponding to oxygen–copper charge transfer. The optical absorption spectra of the solid solutions  $\text{Zn}_{1-x}\text{Cu}_x\text{O}$  ( $x = 0.05, 0.1$ ) and  $\text{Zn}_{0.8}\text{Cu}_{0.2}\text{O}$  also contain an absorption band at 600 nm belonging to the  $d-d$  transitions of  $\text{Cu}^{2+}$ . In addition, these spectra contain an absorption band at 440–470 nm corresponding to the  $\text{Cu}^{2+}$ – $\text{Cu}^+$  transition. The optical absorption intensity of this band increased with the concentration of copper in the solid solutions pointing to the enhancement of  $\text{Cu}^+$  concentration in the samples. This result correlates with a reduction of the intensity of the lines from electrons in the region of small donors in the EPR spectra and confirms the supposition that copper serves as electron trapping sites.

The photocatalytic activity of the  $\text{Zn}_{1-x}\text{Cu}_x\text{O}$  samples was analyzed in the oxidation of hydroquinone upon irradiation of its aqueous solutions at  $\lambda_{\text{max}} = 253$  and 460 nm. Figure 4 demonstrates the dependences of the degree of hydroquinone transformation into *p*-benzoquinone on the catalyst composition upon photoexcitation with visible light for 10 h. Under such conditions, CuO produced by the thermolysis of  $\text{Cu}(\text{HCOO})_2 \cdot 2\text{H}_2\text{O}$  did not exhibit any catalytic activity. Thus, the introduction of small copper amounts (to 5%) into nanodispersed ZnO considerably increases its catalytic efficiency in oxidation reactions.

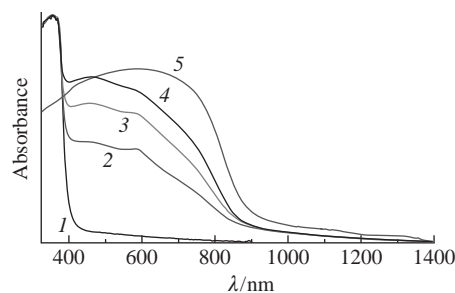


**Figure 3** Optical absorption spectra of  $\text{Zn}_{1-x}\text{Cu}_x\text{O}$ :  $x$  is (1) 0, (2) 0.02, (3) 0.1, (4) 0.2, and (5) 1.

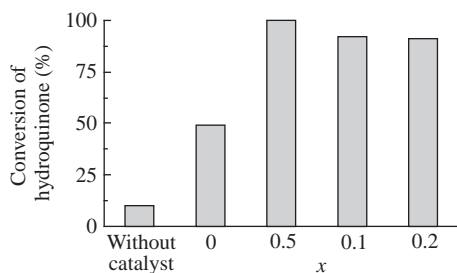


**Figure 4** Degree of hydroquinone conversion in blue light versus the composition of  $Zn_{1-x}Cu_xO$  catalyst.

When the concentration of copper in the  $Zn_{1-x}Cu_xO$  samples was increased to  $x \leq 0.1$ , the catalyst photoactivity decreased, on average, by 10%. Reduction in effective photocatalysis with raising the total copper content was noted in a study of the oxidation power of ZnO/CuO hybrid nanomaterials.<sup>15</sup> This phenomenon was attributed to the enhanced recombination of photogenerated electrons and holes when their total amount increased sharply.

Thus, the use of the mixed formate  $Zn_{1-x}Cu_x(HCOO)_2 \cdot 2H_2O$  ( $0 < x \leq 0.2$ ) as a precursor makes it possible to obtain both the solid solutions  $Zn_{1-x}Cu_xO$  ( $0 < x \leq 0.1$ ) and the hybrid materials  $Zn_{1-x}Cu_xO : CuO$ , which are nucleus-shell composites. It was found that the efficiency of  $Zn_{1-x}Cu_xO$  photocatalysts is determined by the concentration of copper, which serves as an electron acceptor at its content higher than 10%. This process and the presence of intrinsic defects formed in the course of synthesis, which serve as recombination centers, decrease the photoactivity of the samples.

This work was supported in part by the Federal Agency for Scientific Organizations of Russia, the Ural Branch of the Russian Academy of Sciences (project no. 15-6-3-20) and the Russian Foundation for Basic Research (project no. 15-03-02908-a).

## References

- 1 K. Hou, Z. Gao, M. Da, Z. Li, H. Sun, L. Li, Y. Xie, T. Kang and A. Mijit, *Mater. Res. Bull.*, 2012, **47**, 1010.
- 2 R. Singh, *J. Magn. Magn. Mater.*, 2013, **346**, 58.
- 3 B. B. Straumal, A. A. Mazilkin, S. G. Protasova, S. V. Stakhanova, P. B. Straumal, M. F. Bulatov, Th. Tietze, E. Goering and B. Baretzky, *Rev. Adv. Mater. Sci.*, 2015, **41**, 61.
- 4 X. Feng, *J. Phys.: Condens. Matter*, 2004, **16**, 4251.
- 5 M. Yang, G. Pang, L. Jiang and S. Feng, *Nanotechnology*, 2006, **17**, 206.
- 6 O. I. Gyrdasova, V. N. Krasil'nikov, M. A. Melkozerova, E. V. Shalaeva, E. V. Zabolotskaya, L. Yu. Buldakova, M. Yu. Yanchenko and V. G. Bamburov, *Dokl. Chem.*, 2012, **447**, 258 (*Dokl. Akad. Nauk*, 2012, **447**, 292).
- 7 M. A. Melkozerova, V. N. Krasil'nikov, O. I. Gyrdasova, E. V. Shalaeva, I. V. Baklanova, L. Yu. Buldakova and M. Yu. Yanchenko, *Phys. Solid State*, 2013, **55**, 2459 (*Fiz. Tverd. Tela*, 2013, **55**, 2340).
- 8 R. Vogel, P. Hoyer and H. Weller, *J. Phys. Chem.*, 1994, **98**, 3183.
- 9 R. Mohan, K. Krishnamoorthy and S.-J. Kim, *Solid State Commun.*, 2012, **152**, 375.
- 10 U. R. Pillai and S. Deevi, *Appl. Catal., B*, 2006, **64**, 146.
- 11 A. Janotti and C. G. Van de Walle, *Phys. Rev. B*, 2007, **76**, 165202.
- 12 L. S. Vlasenko, *Appl. Magn. Reson.*, 2010, **39**, 103.
- 13 V. A. Nikitenko, in *Zinc Oxide – A Material for Micro- and Optoelectronic Applications*, eds. N. H. Nickel and E. Terukov, Springer, Dordrecht, 2005, p. 69.
- 14 Ya. G. Klyava, *EPR-spektroskopiya neuporyadochennykh tverdykh tel (EPR Spectroscopy of Disordered Solids)*, Zinatne, Riga, 1988 (in Russian).
- 15 A. Samad, M. Furukawa, H. Katsumata, T. Suzuki and S. Kaneco, *J. Photochem. Photobiol. A*, 2016, **325**, 97.

Received: 10th October 2016; Com. 16/5068